Published in final edited form as:
Semin Nucl Med. 2006 January ; 36(1): 36–50.

Future Direction of Renal PET

Zsolt Szabo, MD, PhD,
Division of Nuclear Medicine, Johns Hopkins University School of Medicine

Jinsong Xia, MD, PhD,
Division of Nuclear Medicine, Johns Hopkins University School of Medicine

William B. Mathews, PhD, and
Division of Nuclear Medicine, Johns Hopkins University School of Medicine

Phillip R. Brown, DVM
Department of Comparative Medicine, Johns Hopkins University School of Medicine

1. PET Images as Biomarkers

Biomarkers are biological characteristics that can be used as indicators of normal and pathological processes and they can serve as probes of pharmacologic response to treatment (1). Biomarkers may be utilized at all stages of disease including screening, early diagnosis, prognosis, assessment of disease progression, assessment of disease regression and measurement of drug effects. *Surrogate endpoints* are biomarkers that are used as substitutes for clinical end points. Due to their quantitative character, PET studies of the function and molecular composition of the organs are well suited to be biomarkers. As any biomarker, new PET methods must go through established developmental phases that include discovery, preclinical research, clinical testing and commercial establishment. PET imaging methods for renal imaging are currently in either the discovery or preclinical research phases.

The steps involved in the development of a new renal PET imaging method are analogous to the steps of biomarker development. The first important question to address is which characteristics of the organ, i.e. functional or molecular, should be the focus of imaging? If the goal is to image renal blood flow, the best available tracer and imaging protocol to do this should be selected. The method has to be validated in the preclinical as well as in the clinical setting to insure that it provides reliable, reproducible, quantitative information that is diagnostically useful. On the other hand, if the goal is imaging of molecular targets, such as the level of expression of receptors, the important questions are, which proteins are significantly altered in specific diseases and in which diseases is a specific protein altered in a consistent fashion? Is the molecular target expected to provide disease specific information and will it be helpful to guide treatment?

Gamma camera studies of the kidneys have a long history. Recently magnetic resonance imaging (MRI) and computerized tomography (CT) have adopted imaging protocols and data processing algorithms that were originally developed in nuclear medicine (2,3). The development of clinical PET imaging of the kidneys has been slow. This is in part due to the success of single photon renal imaging, planar or tomographic, and in part due to the usefulness of other noninvasive imaging modalities such as ultrasound, magnetic resonance angiography and CT angiography.

Address: Zsolt Szabo, MD, PhD, Professor, Russell H. Morgan Department of Radiology and Radiological Sciences, Division of Nuclear Medicine, The Johns Hopkins Medical Institutions, 601 N. Caroline Street, Baltimore, MD 21287, USA Room, # JHOC 3233, Email: zszabo@jhmi.edu.

2. Physics and Instrumentation

Multiple PET methods have been applied for performance of physiological and pharmacological studies in humans or experimental animals. This section will review the developments of functional and molecular renal PET imaging and discuss those aspects of PET and renal imaging that are being considered for clinical applications. Positron emission tomography has achieved a high level of technological perfection due to the improvements in detector technology, computer hardware and image processing software.

Detector Technology

Bismuth germanate detectors have replaced NaI(Tl) detectors. Other competitive detector materials, including lutetium oxyorthosilicate that result in shorter deadtimes and improved countrate responses have emerged (4). The faster detector response has been further boosted by higher light output which can be of particular use for blood flow studies of the kidneys with short-lived isotopes such as Rb-82. To take advantage of the high signal density, data acquisition boards have been improved and have been enhanced with powerful reconstruction processors and graphics boards (5). Iterative reconstruction algorithms are continually being improved. Image optimization is achieved using algorithms that are based on statistical principles and take into account the response characteristics of detector systems (6,7).

In comparison to SPECT, PET offers multiple advantages for imaging the kidneys. PET has a tomographic spatial resolution similar to the thickness of the renal cortex, an excellent method for attenuation correction, and a very effective way to correct for scatter. Improved image reconstruction also helps reduce artifacts arising from high radioactivity concentrations in the renal collecting system. PET images can be expressed in SI units (MBq/mL; KBq/mL/MBq injected dose), MKS units (ng/mL), pharmacological units (mEq/mL) or the clinically established SUV values. These properties of PET make quantification of renal blood flow and glomerular filtration rate (GFR) straightforward and also make quantitative imaging of molecular targets possible.

Three types of PET imaging systems devices are available today: 1) small animal PET scanners to image mice and rats, 2) PET scanners and 3) hybrid PET/CT systems to image larger animals and humans. A significant step forward was made with the introduction of hybrid PET/CT imaging systems. PET/CT merges the benefits of two imaging modalities. PET provides the high sensitivity and quantitative accuracy required for molecular and functional imaging, while CT provides tomographic images with the spatial resolution necessary for accurate localization of lesions (4,8). Combination of molecular PET imaging with renal CT arteriography has the potential to improve the diagnosis of renovascular hypertension. The accuracy of CT angiography to detect renal artery stenosis is very high (9–11). PET radioligands have to be developed that will provide complementary information about tissue viability and the adaptive molecular processes that arise in chronic and repetitive hypoxia.

The introduction of inexpensive computers with high computational speeds and storage capacities has contributed significantly to the clinical acceptance of PET. Further improvement of iterative reconstruction methods will have an impact on PET imaging studies of the kidneys since the artifacts caused by high variance in the regional distribution of the radiotracer can be corrected. These methods will also make it possible to quantitatively model the data and minimize attenuation and scatter.

Radioisotopes

Multiple positron emitting radioisotopes can be used for renal imaging. Rubidium-82 is a generator product with a very short half life and relatively high positron energy. Images

obtained with Rb-82 are unfavorably affected by rapid decay and by the increased positron range caused by high positron energy.

Carbon-11 has been extensively used for studies of the heart and brain and most recently also for molecular imaging of the kidneys. Since carbon-11 is chemically identical to stable carbon, its introduction into radiopharmaceutical molecules will not alter their chemical and biological properties. The short half life of 20 minutes may prevent a widespread clinical application of radiopharmaceuticals labeled with carbon-11.

Fluorine-18 has a longer T1/2 (110 min) and is well suited for molecular imaging studies. The longer half-life also permits synthetic procedures of longer duration and F-18 labeled radiopharmaceuticals can be used for receptor binding studies that require longer time periods between injection and imaging. Fluorine-18 also has relatively low positron energy; the shorter positron range will further contribute to better image quality.

Less frequently used positron emitting radioisotopes are gallium-68, copper-62 and 64, N-13 and Co-55 [Table 1]. Copper-62 is a generator product with a half life of 9.8 min that may become clinically useful in the future.

Image Processing

Research PET studies of the kidneys require placement of an arterial catheter to collect the input function which is needed for estimation of radioligand kinetic parameters from tissue time activity curves. For routine clinical applications it will be very important to develop methods in which the arterial input function will be replaced by time activity curves derived from the aorta (12). To equate total blood activity with plasma activity, radiotracers will be needed that have slow metabolism and insignificant uptake into circulating blood cells.

Tracer kinetic models are used to quantify the uptake and release of radioligands in the kidney and other parenchymal organs. Ideally, quantitative parameters of these models reflect physiological variables such as renal blood flow, glomerular filtration or receptor density. The basic operational equation that describes the tissue concentration of the radioligand in the renal parenchyma is a convolution integral of the arterial input function with the tissue impulse response function of the radioligand. Ethylene-diamine tetraacetic acid (EDTA) labeled with positron emitting isotopes Co-55 or Ga-68 is excreted into the renal tubules by glomerular filtration and its kinetics are described by a noncompartmental (nondeterministic or stochastic) impulse response function identical to the impulse response function. This is identical to the impulse response function of Tc-99m DTPA that has been extensively studied in the past (13–15). The glomerular filtration rate can be measured with Ga-68 EDTA/PET and can also be displayed as a parameteric image. The glomerular filtration rate obtained with Ga-68 EDTA normalized to 100 g renal mass was 58 ml/min in a young subject and 30 ml/min/100 g in older subjects (16).

The kinetics of freely diffusible tracers and radioligands that bind to molecular recognition sites can be described by compartmental (deterministic, non-stochastic) impulse response functions (17). Using these kinetic models, exact parameter estimation is achieved by nonlinear least squares curve fitting. Full compartmental models are too cumbersome for practical applications. Graphical methods are simpler and more applicable to everyday situations. They can provide quantitative parametric images within reasonable computational times. Tracers with shorter tissue residence times (reversible binding) are typically quantified by the Logan graphical technique which results in parametric images of distribution volumes DV (18). Reversibility is either attained by backflow of the tracer into the circulation (example: O-15 labeled water) or by excretion of the tracer into the tubular system (example: Co-55 labeled EDTA (19)). Accumulation of radioligands with slow dissociation from binding sites

(irreversible binding) is quantified with the Gjedde-Patlak graphical method (20,21) (example: C-11 L-159,884 a radioligand used for imaging the angiotensin AT1 receptor (22)).

3. Functional Imaging

Category I and II Tracers

Functional PET imaging studies of the kidneys are currently being performed for research purposes and measurements of renal blood flow and glomerular filtration function are well established. Tracers used for perfusion imaging belong to two categories (23): category I tracers such as O-15 labeled water are freely diffusible between tissue and blood; category II tracers such as Rb-82, N-13 ammonia and Cu-62 PTSM are physiologically retained in the tissue.

Renal Blood Flow

The kinetic model of O-15 water is based on the assumptions that all activity is extracted by the parenchyma, extraction is very rapid, and tubular transport has not started or is insignificant at a level that does not influence the calculation of renal blood flow. Parametric images can be obtained using the aorta for estimation of the input function [Figure 1] (12). O-15 has a very short half-life and its production requires the availability of a medical cyclotron. The significance of O-15 labeled water for research studies of the kidneys will probably increase in the future but its wide clinical application is unlikely. The renal blood flow normalized to 100 g tissue measured with O-15 water was 340 mL/min/100g in healthy individuals. In a group of patients with renal dysfunction the renal blood flow was 210±110 mL/min/100g (12). Glomerular filtration represents 20 % of the total renal blood flow, thus, these values are in good agreement with the glomerular filtration rates obtained with Ga-68 EDTA.

Rubidium-82 has a much better chance for clinical utilization. Rubidium-82 is a generator produced potassium analog with a half-life of 75 seconds. It demonstrates high first pass extraction (> 80 %) and slow washout in the kidneys (24). It can therefore be considered a category II tracer and renal blood flow can be calculated using a (modified) microsphere model. A simplified model has been proposed when the tracer is administered by continuous infusion, an equilibrium state is reached and the tissue/blood activity is used to assess renal blood flow. This simplified method requires only one blood sample per measurement and is particularly practical for serial measurements. It has been applied in animal models of renal artery obstruction, occlusion and reperfusion (25).

Copper(II)-pyruvaldehyde bis (n-4-methylthiosemicarbazone) (Cu-PTSM) is another Category II tracer that is labeled with the positron emitting isotopes of copper, Cu-64 or Cu-62. Cu-PTSM could be used in the clinical setting to image both myocardial and renal blood flow. Since the extraction fraction of Cu-PTSM is high and its tissue clearance is slow, the modified microsphere model is applied for quantification. Renal blood flow measured with Cu-PTSM correlated well with the renal blood flow obtained with radioactive microspheres (26,27). In rats, comparison studies with Co-57 labeled 15 μm microspheres yielded an apparent renal extraction fraction of 93 % and an apparent myocardial extraction fraction of 62% (28). Both values were higher than the extraction fraction values measured during first pass (hence the expression apparent extraction fraction) which indicated that recirculation of the tracer had occurred. In dogs, renal cortical blood flow determined with Cu-PTSM was 300-550 mL/min/100g and correlated well with the blood flow values determined with the reference microsphere method (27). Correlation between flow values determined with Cu-PTSM and microspheres is much better in the renal cortex than the medulla, an effect which can result not only from the partial volume effects with PET but also from the documented underestimation of medullary flow by microspheres (27).

N-13 labeled ammonia has also been used for imaging both myocardial and renal perfusion (19). Parametric images are obtained with the pixel based Gjedde-Patlak plot (17,21). Extraction occurs in two steps, from blood to a more reversible compartment and then from this more reversible to an irreversible compartment (19). Despite the presence of a reversible compartment, the renal extraction of this tracer is nearly 100 %. The renal blood flow measured with N-13 ammonia in dogs was 400 mL/min/100g and correlated well with renal blood flow values obtained with O-15 water (19). N-13 ammonia can be used in patients at research institutions equiped with a medical cyclotron (29).

In summary, renal blood flow studies in humans with PET are feasible. Some tracers such as O-15 water and N-13 ammonia, will likely remain research tools, others, such as Rb-82 and Cu-PTSM have a good chance of clinical utilization. Potential applications include measurements of renal blood flow in renovascular disease, in rejection or acute tubular necrosis of transplanted organs, in drug induced nephropathies, ureteral obstruction, before and after revascularization, and before and after placement of ureteral stents.

Glomerular Filtration

Glomerular filtration has been imaged and quantified in experimental animals using PET and either gallium-68 EDTA or cobalt-55 EDTA as radiotracers. (30). Human studies have not been reported with cobalt-55 EDTA but renal function has been studied in healthy human subjects using Ga-68 EDTA. Organ activity was corrected for blood content using $C^{15}O$ gas which binds to circulating red blood cells. The renal blood volume was 19 ml/100 g for a younger (21 years old) subject and 12 ml/100 g for older (65–77 y) subjects. The glomerular filtration rate was 57.8 ml/min/100 g for the 21 years old subject and 30.4 ml/min/100 g for the older subjects (16). If multipled by 5 to correct for glomerular blood flow contribution, these values are comparable to the renal blood flow measurements.

The most important clinical application for imaging glomerular function with PET would be the captopril test in renovascular hypertension. Some technical difficulties related to that test such as the effect of background activity could be easily resolved since PET images are virtually background free. Furthermore, the postulated uncoupling of glomerular filtration from renal perfusion after administration of an angiotensin converting enzyme inhibitor (ACEI) or an angiotensin receptor blocker (ARB) (31) could be better quantified. Subtle changes of renal perfusion or glomerular function with exercise (32) or after aspirin (33) administration could also be exactly quantified.

4. Molecular Imaging

Molecular imaging is the hallmark of the rapidly expanding area of clinical PET/CT. PET studies have been successfully used as surrogate endpoints in the management of cancer and ischemic heart disease. Molecular imaging of the kidneys with PET is rather limited. The following list shows some potential applications of renal molecular imaging, the emphasis being on *in vivo* imaging:

- Regulation of the receptors, enzymes, membrane transporters and signal transduction proteins in physiology and renal diseases
- Tissue hypoxia and apoptosis in renovascular renal disease and obstructive nephropathy
- Monitoring of the molecular signatures of atherosclerotic plaques
- Endothelial dysfunction and response to balloon revascularization and restenosis

- Early molecular assessment of the nephrotoxic effects of cyclosporine, anticancer drugs and radiation therapy
- Imaging of renal and prostate carcinoma, primary tumor detection and assessment of the potential for metastatic spread
- Kinetics of drug delivery systems based on the organic anion or cation transporters, glucose transporters or peptide transporters
- Delivery and deposition of prodrugs
- Reporter gene technology and delivery of gene therapy (nuclear and mitochondrial).
- Monitoring gene therapy of renal diseases including transplant rejection and ischemia reperfusion injury.
- Assessment of the delivery of cellular, viral and non-viral vectors (liposomes, polycations, fusion proteins, electroporation, hematopoietic stem cells)
- Stem cell kinetics including local presence, bloodborn migration, activation, seeding and role in renal remodeling (physiological, pathological and therapy induced).
- Role of receptors and oncoproteins in cellular proliferation, apoptosis, tubular atrophy and interstitial fibrosis.
- Monitoring ras gene targeting in kidney diseases
- Assessment of cell therapy devices (bioartificial filters, renal tubule assist devices) and, ultimately, of bioartificial kidneys.
- Targeting of signal transduction molecules with growth factors and cytokines.

The above list may sound overly optimistic today, but it is certain that radioisotope imaging in general, and PET imaging in particular, offers advantages that will lead to their increasing role in molecular nephrology. The subsequent paragraphs describe the present status of molecular renal imaging including targeting of metabolism, transporters and receptors.

Metabolism

Imaging metabolism can be regarded as a form of functional imaging because it measures an important functional aspect of an organ and the tracer is a substrate that undergoes metabolic changes. Metabolic imaging can also be categorized as a form of molecular imaging because the radiotracer to be metabolized has to first undergo protein-ligand interactions. The proteins to which the tracer binds are membrane transporters and the enzymes involved in the metabolic process. Available imaging methods include studies of the citric acid cycle with C-11 labeled acetate and glucose metabolism with sugar analogs.

Of particular interest for renal imaging is Carbon-11 acetate which is a probe of citric acid cycle flux and oxidative metabolism. After intravenous administration Carbon-11 acetate demonstrates prompt uptake in the kidneys, which results in excellent images. The metabolic product carbon-11 dioxide is cleared from the renal parenchyma by way of circulation. C-11 acetate has been used in patients with parenchymal renal disease and hemodynamically significant renal artery stenosis (34). A linear correlation between the renal uptake (K_1) and release (k_2) has been described in normal kidneys and kidneys with stenosed arteries, in diabetic nephropathy, hypertensive nephropathy and membranous glomerulonephritis. Disassociation of the kinetic parameters (k_2 decreased to larger degree than K_1) has been found in renal cell carcinoma. This dissociation results in high tumor-to-non-tumor ratios and makes possible to delineate renal cancer from normal kidney tissue (34).

Carbon-11 acetate is not excreted into urine and this property has been utilized to image prostate cancer. The diagnostic accuracy of carbon-11 acetate PET in prostate cancer is higher than the accuracy of [^{18}F]FDG PET (35) and is similar to carbon-11 choline PET (36). The effective radiation dose from C-11 acetate is clinically acceptable; the critical organ is the pancreas with an absorbed dose of 0.017 mGy/MBq (37).

Membrane Transport

Peptide Transporters—Proton-coupled di/tri-peptide transporters are localized at the brush-border membranes of intestinal and renal epithelial cells. PepT1 is exclusively expressed in the small intestine, whereas both PepT1 and PepT2 are expressed in the kidneys. PepT1 localizes to segment S1 of the proximal tubule and PepT2 localizes to segments S2 and S3. PepT1-mRNA is predominantly found in the renal cortex while PepT2-mRNA resides in the outer medulla (38).

Peptide transporters play important physiological roles in protein absorption and amino acid homeostasis. They are also involved in the transport of orally active peptide-like drugs such as the beta-lactam antibiotics, bestatin, ACE inhibitors and renin inhibitors (39,40). Studies of receptor-mediated regulation have shown that PepT1-mediated transport is up-regulated at the level of gene transcription in response to fasting and starvation and by exposure to receptor agonists such as EGF, insulin, leptin, and clonidine (41).

Because they interact with a broad array of substrates, PepT1 and PepT2 transporters are not drug targets per se but they have proved to be relevant at the level of drug transport. They are involved in the uptake of prodrugs of aciclovir and ganciclovir and are major target for development of novel drug delivery systems. Targeted prodrug design represents a new strategy for directed and efficient drug delivery. Targeting the prodrugs to a specific enzyme or a specific membrane transporter, or both, has the potential to be a selective drug delivery system (39).

A series of dipeptide derivatives have been synthesized as competitive inhibitors of the PepT2 transporter (42). The dipeptide Gly-Sar has been radiolabeled with carbon-11 for functional imaging of the renal PepT2. C-11 Gly-Sar could be used to probe the renal pharmacokinetics of drugs (38). The micro PET images obtained with C-11 Gly-Sar show accumulation of this radioligand in the renal medulla [Figure 2], a distribution different from other radiotracers that typically accumulate in the renal cortex.

Organic Cation and Anion Transporters—Transporter imaging with radionuclides has been used for a long time in renal diseases. Radioiodine labeled ortho-hippuric acid and Tc-99m mercaptoacetyltriglyceride (MAG3) have been used extensively as substrates of the organic anion transporter. A second class of single photon radiopharmaceuticals is represented by Tc-99m diaminocyclohexane (DACH), which is a substrate of the organic cation transporters (43).

Of potential interest for PET imaging studies are macrocyclic compounds that are the analogs of cyclen and cyclam [Scheme 1]. Replacement of the four displayed hydrogens in cyclen results in the chelator DOTA while replacement of the hydrogens in cyclam results in the chelator TETA. DOTA, TETA and other macrocycles have been used as chelators for radioactive metals. Examples are gallium-68 labeling of a somatostatin analog for tumor receptor imaging (44) or rhenium 188 and 186 for targeted radiotherapy (45).

Macrocycles have also been investigated as chelators of copper isotopes suitable for PET imaging. The biodistributions of these Cu-64-labeled complexes depended on the the size of the macrocycle backbone and the formal charge of the complex. All compounds showed uptake

and clearance through the liver and kidneys; however, the positively charged Cu-64 complexes showed significantly higher uptake in both of these organs than did the negatively charged or neutral complexes (46).

Copper-64 macrocycles have been evaluated as substrates for the organic anion transporter for potential use as a diagnostic tool for Dubin-Johnson's syndrome. Small animal studies indicated that the cMOAT was involved in the excretion of the Cu-64 complex of compound 5 (47). A gene mutation of this organic anion transporter appears to cause Dubin-Johnson syndrome in humans (48). It is plausible that radiometal chelating macrocyclic compounds that are substrates of the renal organic transporters will be designed in the near future.

Sun et al. synthesized three monooxo-tetraazamacrocyclic ligands with a cyclam backbone, that had different ring sizes and oxo group positions (49). While the exact mechanism of their accumulation in the kidneys has yet to be investigated, they all demonstrated significant accumulation in the renal cortex [Figure 3].

Glucose Transporters—Two major classes of glucose transporters present in the renal tubular cells are the GLUT and the SGLT. The members of the GLUT glucose transporter family are ATP-independent facilitative transporters which catalyze the transport of glucose down its concentration gradient. Several glucose transporters have been identified in the kidneys including the isoforms GLUT1, 3 and 4. A different class of transporters, the sodium dependent glucose transporter (SGLT) is ATP-dependent and can transport glucose against its concentration gradient. Both transporter types can be saturated under normal glucose conditions (50).

Fluorine-18 labeled FDG (fluoro-deoxyglucose) is the most important substrate of the GLUT transporter family that has been introduced for PET imaging. F-18 FDG is not appropriate for imaging glucose kinetics in the kidneys because it is excreted into the tubular lumen and accumulated in the renal collecting system.

The sodium dependent glucose transporter (SGLT) class is responsible for reuptake of glucose from the filtrate in the proximal tubules. (The same type of glucose transporter is also responsible for uptake of glucose in the small intestine). The most important subtypes are SGLT1, SGLT2, and SGLT3 (51).

Methyl-D-glucoside is a substrate of SGLT. Carbon-11 labeled methyl-α-D-glucoside accumulates in the renal cortex that contains S1 and S2 segments of proximal tubules (52). The beta isomer, 2′-[^{18}F]fluoroethyl-β-D-glucoside accumulates in the outer medulla, a kidney region that contains the S3 segments of renal proximal tubules (53). Both radioligands are potentially useful for molecular imaging of the kidneys in diabetes mellitus. Glucosides have been studied as drug delivery vectors to the kidneys (54) and the SGLT is being investigated as a molecular target of anti-diabetic drugs. Imaging will certainly play a role in monitoring this form of drug delivery.

Enzymes

The best known proteins of the renin angiotensin system that could be targets of imaging are the angiotensin converting enzyme (ACE), renin and the angiotensin receptors. Fluorine-18 labeled captopril was the first radioligand introduced for PET imaging of the ACE. After intravenous administration to humans, this radioligand showed high specific binding in the lung and kidney (55). A compartmental model of receptor binding has been designed to quantify the binding of F-18 captopril (56,57) and a study has been carried out in humans to determine the dose of ACE inhibitor required to specifically block ACE.

More recently a second ACE inhibitor, (4S)-1-[(S)-3-Mercapto-2-methylpropanoyl]-4-phenylthio-L-proline (zofenoprilat), the active metabolite of the potent ACE inhibitor zofenopril calcium, was labeled with carbon-11. Preliminary PET studies performed in human volunteers showed that the drug accumulated in organs with high ACE levels such as the lungs and kidneys, and in organs involved in drug metabolism such as the liver and gall bladder (58).

The DD variant of the ACE gene polymorphism appears to be associated with increased risk of developing chronic allograft dysfunction (59). In the future, radiolabeled ACE inhibitors will permit quantification of ACE binding of the kidneys with PET and provide imaging insight into this important association.

The Angiotensin AT1R Subtype Receptor (AT1R)

Physiology—Angiotensin II acts on its receptors and the angiotensin receptors are considered to be the central components of the renin-angiotensin system (RAS). In the human body two receptor subtypes of angiotensin II have been identified: AT1R and AT2R. Vasoconstriction, aldosterone release, vasopressin release, sodium reabsorption, water retention and many other physiological effects of angiotesin II are mediated by the AT1R. In addition to its physiological roles, this receptor also plays an important role in postinfarct myocardial remodeling, nephrosclerosis, vascular media hypertrophy, endothelial dysfunction and athero-thrombosis (60).

Before clinical imaging studies are started, it is important to understand to what degree the AT1R is affected by physiological factors. If effects of aging, dietary sodium, sex hormones, stress etc. are all involved in the changes of the AT1R, one or more of these factors may cause difficulty during interpretation of the PET studies. It is known that expression of the AT1R is enhanced by factors that contribute to development of arterial hypertension. These include: dietary sodium (61) which causes hypertension in salt sensitive subjects, hypercholesterolemia (62) which can result in arteriosclerosis and increased arterial wall stiffness, and renal hypoxia (63) which will lead to renovascular hypertension. The AT1R is modulated by stress hormones and sexual hormones as well (64,65) and there is evidence that post-ovarectomy (and likely post-menopausal) hypertension is linked to increased renal AT1R receptor and salt sensitivity (66). Well controlled human studies need to be designed to separate the changes caused by physiological and pathological variables.

Hypertension—AT1R is upregulated by hyperinsulinism (67) and by elevated LDL (68) and is involved in the development of insulin resistance, metabolic syndrome, hypertension and other disorders associated with increased body weight (69,70). Patients with insulin resistance often develop salt sensitive hypertension. Experimental data indicate that increased expression of the AT1R is associated with the development of hypertension of hyperinsulinemia, an effect that can be prevented by short- and long-term AT1 receptor blockade (70). In a mouse genetic model of metabolic syndrome, treatment with angiotensin receptor blockers inhibited the development of hyperinsulinemia, hypertension, obesity, cardiac hypertrophy, and atherosclerosis (71). In humans, treatment with the angiotensin receptor blocker valsartan decreases the incidence of diabetes in high-risk hypertensive patients (72).

Renal diseases—Expression of renal AT1R is increased in reflux nephropathy (73), myocardial infarction (74), and experimental renovascular hypertension (75). In these disease states, AT1R activation results in vasoconstriction, water and salt retention, accumulation of reactive oxygen species, cellular hypertrophy, hyperplasia and apoptosis. Interventional studies demonstrate that drugs that reduce AT1R activation can improve endothelial dysfunction,

inhibit the onset and progression of atherosclerosis, decrease abnormal arterial blood pressure and protect renal function (76).

Radioligands—Due to the great significance of AT1R, considerable effort has been made for its investigation *in vivo* with PET (77–80). PET is well suited for *in vivo* investigations of AT1R regulation in animals (79,81). Human studies are expected to provide additional important insights into the regulation of the AT1R and elucidation of its role in arterial hypertension, renal diseases and myocardial remodeling. In human arterial hypertension AT1R may be upregulated or may become hyperresponsive by another mechanism (82). Hypertension could result from multiple changes of the renin angiotensin system including an increased total number of receptors, increased number of physiologically active receptors, inappropriate upregulation of receptors in response to sodium intake, stress, altered hormone levels, and increased levels of circulating renin and angiotensin II.

Angiotensin receptor blockers (ARBs) are an important resource for the development of radioligands for PET. Losartan, eprosartan, and telmisartan are competitive, surmountable antagonists which do not impair the maximum response to angiotensin II. Non-competitive, insurmountable ARBs such as candesartan, valsartan and irbesartan decrease the sensitivity of the receptor and also reduce its maximal response to agonist stimulation (83). Radiolabeled insurmountable antagonists are suited for single time point organ imaging or whole body PET imaging. Their binding can be quantitatively analyzed by the Gjede-Patlak ploit (22). An example of an insurmountable antagonist for PET is C-11 L-159,884 or N-[[4′-[(2-ethyl-5,7-dimethyl-3H-imidazo[4,5-b]pyridin-3-yl)methyl][1,1′-biphenyl]-2-yl]sulfonyl]-4-methoxybenzamide [Scheme 2] (84).

Tissue accumulation and receptor binding of surmountable antagonists is best analyzed by the Logan plot and quantified by the distribution volume *DV* or binding potential *BP*. An example is 2-Butyl-5-methoxymethyl-6-(1-oxopyridin-2-yl)-3-[[2-(1H-tetrazol-5-yl)biphenyl-4-yl] methyl]-3H-imidazo[4,5-b]pyridine (KR-31173), the newest ligand that has been radiolabeled with carbon-11 for imaging the AT1R with PET [Scheme 2]. KR-31173 is a derivative of the potent AT1R antagonist SK-1080 (85,86). Specific binding of this radioligand in the adrenals, kidneys, lungs and heart of rodents is 90% (78).

PET Imaging of Physiologic Receptor Regulation—Multiple imaging studies have been carried out with both C-11 L-159,884 and C-11 KR 31173. These studies showed that renal imaging more successful with C-11 L-159,884 in dogs and more successful with C-11 KR 31173 in nonhuman primates. First studies (Szabo group, unpublished) in humans with C-11 KR31173 are encouraging. The AT1R of the kidneys and left adrenal were clearly visualized in dogs but high liver uptake interfered with the display of the right adrenal gland. Antagonist inhibition studies showed 60 % specific binding in the kidneys. Patlak analysis of the renal time activity curves revealed 67 % specific binding (22).

Carbon-11 L-159,884 has been used for investigation of receptor regulation *in vivo* in dogs. In a sequence of experiments it was shown that both the cortical (predominantly glomerular) and the medullary (predominantly tubular) AT1R was upregulated by increased dietary sodium. In the renal cortex, *ex vivo* receptor quantification data correlated well with the *in vivo* PET data (79). With the presently available image resolution and image processing, quantification of the tubular AT1R was not possible. In a second study the effect of estrogen hormone substitution was investigated in ovarectomized dogs. It was found that estrogen substitution downregulated and estrogen deficiency upregulated the AT1R. *In vitro* tissue binding data correlated well with the *in vivo* data obtained with PET (87). In both physiological perturbation models of AT1R regulation a negative correlation between AT1R status and renin activity was measured,

providing first time by means of *in vivo* PET the molecular foundation of Arthur C. Guyton's concept of negative feedback regulation of arterial blood pressure (88).

Model of Renovascular Hypertension—The results of the above described physiological paradigms are quite different from those obtained with the animal model of renovascular hypertension. We measured the left to right retention ratio of C-11 L-159,884 at 55–95 minutes post intravenous tracer administration in two sham operated dogs and in four mongrel dogs in which left sided renal artery stenosis was created with an ameroid occluder. In the sham operated animals the left-to-right binding ratio was close to 1. PET showed that in dogs renal artery stenosis resulted in reduced renal blood flow, reduced radioligand delivery but increased radioligand retention [Figure 4].

In the four dogs on a well controlled daily sodium intake 3 weeks after placement of ameroids on the left renal artery the left-to-right ratio was significantly increased consistent (1.43) with an increased receptor binding in the stenotic kidney [Figure 5 left hand graph]. This increased AT1R binding correlated positively with increased plasma renin activity [Figure 5 right hand graph]. This positive correlation between receptor binding and renin activity was conistent with the concept of a positive feedback mechanism, which leads to the development of arterial hypertension in a pathological paradigm. It will be interesting to perform PET studies in humans and correlate the findings of receptor binding with plasma renin activity to establish whether or not the same concept is valid in humans. Another important study group will be subjects who have salt sensitivity hypertension. As mentioned in the previous paragraphs, salt sensitivity hypertension has been observed in metabolic syndrome and post-ovarectomy. It will be very interesting to corroborate whether a loss of a negative feedback between renin activity and AT1R can be observed in such individuals similarly to renovascular hypertension.

In dogs with experimental renal artery stenosis, receptor binding was almost completely normalized three months after placement of the ameroid. Autopsy revealed extensive collaterals in the area of the capsular arteries of the stenotic kidneys and this could explain the compensatory increase in perfusion and normalization of AT1 receptor expression. This finding could be of particular significance for similar studies performed in humans with renovascular hypertension since it indicates that: 1) the AT1R may be a sensitive probe of renal ischemia; and 2) if an equilibrium between organ oxygen demand (atrophy) and blood supply (collaterals) develops AT1R protein expression may return to normal levels. An important application would be assessment of the significance of renovascular hypertension by means of molecular imaging, another would be the assessment of the beneficial effects of arterial revascularization.

In renovascular hypertension systemic plasma renin activity and systemic angiotensin II levels are increased initially (89,90). No conversion of arterially delivered angiotensin I to angiotensin II has been detected across the renal beds in either essential or renovascular hypertension and, therefore, a high degree of compartmentalization of Ang II in the kidneys has been postulated (91). Some publications describe AT1R up-regulation, some describe no change and others describe AT1R receptor down-regulation in renal hypoperfusion (92), (93) (94). The differences could be caused by the differences in the methods applied (e.g. receptor binding assays vs. mRNA determinations), by differences in the time points of measurement, by the age of the animals included in the experiments (95), or by species differences in AT1R receptor regulation. It is important to emphasize that the differential regulation of AT1a and AT1b receptor subtypes applies only to rodents (93,96–98). Another limiting factor in delineating the role of the AT1R in human renovascular hypertension has been that receptor expression has only been studied only in tissues removed operatively or harvested at post-mortem.

Cardiovascular Diseases—AT1R/PET imaging may not only be important in the kidneys; potential nonrenal applications include investigations of cardiac receptor regulation in cardiovascular diseases. Angiotensin II and its target the AT1R are involved in the regulation of circulating lipids, development of atherosclerosis, tissue response to myocardial ischemia, coronary thrombosis or myocardial infarction and in the molecular mechanisms of arrhythmias, remodeling, ventricular dilatation and heart failure (99). The density of the myocardial AT1R is nearly 20 times lower than the density of glomerular AT1R. This may pose a problem if the degree of upregulation is small or it may represent an advantage if upregulation is significant since it could increase the contrast between pathological and healthy tissues in PET studies.

Imaging of vulnerable atherosclerotic plaques is another potential application of AT1R PET. One recent study demonstrated that components of the RAS, including AT1R, were expressed at strategically relevant sites of human coronary atherosclerotic plaques. Angiotensin II was detected in close proximity to the presumed plaque rupture site in coronary artery sections from patients who died acutely after myocardial infarction. Co-localization of the components of the RAS with interleukin 6 was observed in stable coronary plaques and atherectomy tissues, and angiotensin II induced the expression of interleukin 6 *in vitro*, both in macrophages and in SMC. These findings are consistent with the notion that the RAS may contribute to the inflammatory processes within the atherosclerotic vascular wall and to the development of acute coronary syndromes. (100).

5. Development of Molecular Tracers

The rapid spread of PET and PET/CT imaging can be partially explained by the rapid development of treatment options that are based on molecular pharmacology and the ability of PET to predict and monitor the variance of individual responses to therapy. For PET imaging to expand in nephro-urology, its necessity must be established. Overall, there have been relatively few molecular based PET imaging studies in nephrological and urological diseases. One potential problem is the high background activity by the renal elimination of tracer through the kidneys, ureters and urine. Another technical challenge is caused by difficulties in obtaining reproducible and reliable information about a mobile organ as the kidneys are subject to respiratory movements and they are susceptible to abdominal artifacts. Small lesions may be “blurred” due to respiratory movement.

The previous section described membrane transporter tracers and tracers for receptor imaging. However, new molecular probes that are more disease-specific need be explored.

Gene imaging

With the advent of functional genomics and pharmacogenomics, medicine will shift towards personalized gene-based therapies. There are many effective gene treatment regimens emerging for urological disorders, but most carry significant risks to the patient. The field of PET molecular imaging is rapidly evolving and will permit a meaningful understanding of *in vivo* regulation of vital gene molecular events in real-time.

Recently, a study was performed to monitor experimental gene therapy using PET imaging technology (101). Micro-PET small animal studies with F-18-FHBG (F-18-labeled 9-[4-fluoro-3-(hydroxymethyl)butyl]guanine), a substrate for the sr39TK enzyme, were used to successfully demonstrate the expression of a herpes simplex virus thymidine kinase (HSV1-tk) reporter gene within prostate tumor xenografts. Only the CL1-SR39 tumor xenograft in severe combined immunodeficient (SCID) mice with stable sr39TK expression could be visulaized. Wild-type CL1 tumors that lacked the sr39tk gene needed to convert and retain F-18-FHBG metabolites to a significant degree were not delineated. Both tumor xenografts could be easily imaged with F-18 FDG. This work demonstrates that noninvasive tracking of

the distribution of adenoviral gene delivery is possible and suggests that PET could be used to assess the therapeutic effect and toxicity of gene therapy for nephrological and urological disorders as well.

Ischemic Nephropathy

Patients with ischemic kidney disorders develop loss of renal function in addition to large-vessel occlusive disease (102). Success in managing ischemic nephropathy depends on identification of progressive lesions and on revascularization of critical stenoses before renal parenchymal injury becomes irreversible.

Receptor imaging is already a very successful branch of nuclear medicine and the expectation is that it will be used in ischemic diseases in the future. A clinical PET study was conducted with [^{11}C](R)-PK11195 in a small cohort of patients after ischemic stroke to define the time course of microglial activation (103). PK11195 (1-[2-chlorophenyl]-N-methyl-N-[1-methyl-propyl]-3-isoquinoline carboxamide) is a specific ligand for the peripheral benzodiazepine binding site (PBBS). The PBBS is particularly abundant on activated microglia and other cells of the mononuclear phagocyte lineage. Increased binding of [^{11}C](R)-PK11195 in the post-ischemic period was observed both in the affected zone and in remote areas such as the pons, 3 to 150 days after the infarct. The receptor imaging probe [^{11}C](R)-PK11195 may have promise to assess the effects of pharmacological intervention *in vivo*. With this tracer one could test under which conditions the activation of microglia is potentially deleterious or beneficial for an extended period after the actual stroke event. Similar studies are very likely to be developed for renovascular disease as well. One example is the previously mentioned AT1R.

PET probes targeting the fibrogenic molecular pathways will produce useful information to improve patient selection and make it possible to analyze the risks and benefits of early intervention in atherosclerotic renovascular injury. A major focus of ischemic nephropathy research until now has been on the role of fibrogenic cytokines. The roles of TGF-β and NF-κ in the atherosclerotic disease processes and vascular repair has been studied (102). Meaningful predictors of renal function after revascularization are sparse and such investigation will offer major contributions both in the understanding of the pathophysiology of tissue injury and in clinical outcomes. The monitoring of TGF- β, NF-κ activity during disease development in a real-time manner would be important to validate the efficacy and tissue distribution of potential TGF-β, NF-κ modulating drugs.

PET Imaging of Tumor Hypoxia

The major clinical indications for PET have been in the field of oncology. Renal cell carcinoma accounts for 3% of all cancers in adults and is the most common malignancy of the kidney (104). Kidney cancer is steadily increasing at a rate of about 2.5% per year (105,106).

A variety of solid renal cell carcinomas demonstrate oxygen deficiency as a result of rapid growth and insufficient tumor angiogenesis. Hypoxia appears to accelerate malignant progression and metastatic potental in solid tumors, and consequently leads to resistance against anticancer drugs and decreases response to radiotherapy. Defining hypoxia in tumor tissue is important in optimizing the use and outcome of different therapeutic modalities. Several compounds have been synthesized and tested in animals and humans for this purpose: F-18 Fluoroazomycinarabinofuranoside (FAZA) (107), F-18 fluoromisonidazole (FMISO) (108-110), Cu-60 diacetyl-bis(N4-methylthiosemicarbazone) (Cu-ATSM) (111), F-18 FETNIM (112), 2-(2-nitroimidazol-1[H]-yl)-N-(3-[F-18]fluoropropyl)acetamide (F-18-EF1) (113), F-18 Fluoromisonidazole (FMISO) (114) and F-18 [2-(2-nitro-1[H]-imidazol-1-yl)-N-(2,2,3,3,3-penta-fluoropropyl)-acetamide] (EF5) (115). These compounds diffuse into normally oxygenated and hypoxic cells but are retained in substantially higher concentrations

in the latter tissues, which can be detected by external PET imaging. In a study (107) the uptake of FAZA in hypoxia tissue, a recently developed hypoxia tracer for PET imaging, was compared with an established hypoxia tracer FMISO both *in vitro* and *in vivo*. The data of *in vitro* studies, using Walker 256 rat carcinosarcoma cells, that indicated hypoxia-selective uptake of both FAZA and FMISO in tumor cells were consistent with *in vivo* studies in experimental rat tumors eleven to twelve days after tumor cell implantation. Both compounds tend to accumulate in sites of hypoxia and are therefore rendered suitable for PET imaging of carcinoma. Hypoxia is a profound biologic phenomenon established in all solid renal cell carcinomas. These new PET probes designed to target tumor hypoxia could provide essential information in renal cell carcinoma that may be used for selection of anticancer therapeutic strategies in order to improve overall tumor response.

Angiogenesis

Imaging of angiogenesis, a phenomenon noted in renal revascularization and most malignant processes, may also provide important information in the kidneys. One promising approach involves the assessment of the endothelin (ET) receptors (ETAR and ETBR) with C-11 L-753,037. In humans ET receptors are involved in angiogenesis and are expressed in the heart, brain, lung, kidney, and aorta. L-753,037 has been described as a potent, selective inhibitor of ETA and ETB receptors, with Ki values of 0.034 and 0.104 nmol/L, respectively, using I-125 ET-1 competition binding assays were used in cloned human ETA and ETB receptor preparations (116). The binding of L-753,037 to ET receptors *in vitro* was shown to be reversible and competitive. In a study by our group, L-753,037 was radiolabeled with the positron-emitting radionuclide C-11 and the new radiotracer was evaluated for its binding to ET receptors in mice and a dog. In the dog, a dynamic PET study of the heart showed high tracer accumulation at 55–95 min after injection. Injection of the ETA antagonist L-753,164 30 min before C-11 L-753,037 administration led to a significant reduction in tracer binding. Administration of both ETA (L-753,164) and mixed ETA/ETB (L-753,137) receptor antagonists resulted in dose-dependent inhibition of C-11 L-753,037 binding in mouse kidneys (117).

Cell–cell and cell–matrix interactions play essential roles in renal angiogenesis. Integrins are a family of heterodimeric endothelial cell membrane proteins, which are receptors for extracellular matrix proteins containing the amino acid sequence arginine, glycine, and aspartate (RGD). The integrin $\alpha_v\beta_3$ plays an important role in angiogenesis and is currently being evaluated as a target for new therapeutic approaches. Recently, several techniques are being studied to enable noninvasive determination of $\alpha_v\beta_3$ expression (118). Haubner et al developed a new molecular imaging technique with PET and F-18 Galacto-RGD, a F-18-labeled glycosylated $\alpha_v\beta_3$ antagonist (119). This technique will allow *in vivo* monitoring of $\alpha_v\beta_3$ expression, and can provide important information for planning and monitoring anti-angiogenic therapies targeting the $\alpha_v\beta_3$ integrins. It can also reveal the involvement and role of the integrin family in angiogenic processes in various diseases. Measurements of endothelin receptor and integrins are just a few examples of what can be done using PET. These studies exemplify how the morphology and function of renal angiogenesis can be visualized.

Conclusions

Over 95% of PET procedures performed around the world use FDG as the imaging agent. For PET and PET/CT studies of the kidneys to become clinically useful, new disease-specific molecular probes need to be developed since many nephrological and urological disorders are initiated at the molecular and organelle levels and may remain localized at their origin for an extended period. With the advent of more optimal tracers, PET may serve as an invaluable tool in the diagnosis and management of nephrological and urological disorders. Clearly, the new

approaches mentioned above are at best in an experimental stage and more research will be needed before their clinical implementation.

Acknowledgements

The research related to this publication has been supported by NIH grant number DK-50183.

References

1. Hewitt SM, Dear J, Star RA. Discovery of protein biomarkers for renal diseases. J Am Soc Nephrol 2004;15:1677–1689. [PubMed: 15213255]
2. Lorenz CH, Powers TA, Partain CL. Quantitative imaging of renal blood flow and function. Invest Radiol 1992;27 (Suppl 2):S109–S114. [PubMed: 1468868]
3. Romero JC, Lerman LO. Novel noninvasive techniques for studying renal function in man. Semin Nephrol 2000;20:456–462. [PubMed: 11022899]
4. Townsend DW. Physical principles and technology of clinical PET imaging. Ann Acad Med Singapore 2004;33:133–145. [PubMed: 15098626]
5. Judenhofer MS, Pichler BJ, Cherry SR. Evaluation of high performance data acquisition boards for simultaneous sampling of fast signals from PET detectors. Physics in Medicine and Biology 2005;50:29–44. [PubMed: 15715420]
6. Kontaxakis G, Strauss LG, Thireou T, Ledesma-Carbayo MJ, Santos A, Pavlopoulos SA, Dimitrakopoulou-Strauss A. Iterative image reconstruction for clinical PET using ordered subsets, median root prior, and a web-based interface. Mol Imaging Biol 2002;4:219–231. [PubMed: 14537126]
7. Gutman F, Gardin I, Delahaye N, Rakotonirina H, Hitzel A, Manrique A, Le Guludec D, Vera P. Optimisation of the OS-EM algorithm and comparison with FBP for image reconstruction on a dual-head camera: a phantom and a clinical 18F-FDG study. Eur J Nucl Med Mol Imaging 2003;30:1510–1519. [PubMed: 14579091]
8. Koepfli P, Hany TF, Wyss CA, Namdar M, Burger C, Konstantinidis AV, Berthold T, von Schulthess GK, Kaufmann PA. CT attenuation correction for myocardial perfusion quantification using a PET/CT hybrid scanner. J Nucl Med 2004;45:537–542. [PubMed: 15073247]
9. Kaatee R, Beek FJ, de Lange EE, van Leeuwen MS, Smits HF, van der Ven PJ, Beutler JJ, Mali WP. Renal artery stenosis: detection and quantification with spiral CT angiography versus optimized digital subtraction angiography. Radiology 1997;205:121–127. [PubMed: 9314973]
10. Kim TS, Chung JW, Park JH, Kim SH, Yeon KM, Han MC. Renal artery evaluation: comparison of spiral CT angiography to intra-arterial DSA. J Vasc Interv Radiol 1998;9:553–559. [PubMed: 9684822]
11. Carlos RC, Axelrod DA, Ellis JH, Abrahamse PH, Fendrick AM. Incorporating patient-centered outcomes in the analysis of cost-effectiveness: imaging strategies for renovascular hypertension. AJR Am J Roentgenol 2003;181:1653–1661. [PubMed: 14627591]
12. Alpert NM, Rabito CA, Correia DJ, Babich JW, Littman BH, Tompkins RG, Rubin NT, Rubin RH, Fischman AJ. Mapping of local renal blood flow with PET and H(2)(15)O. J Nucl Med 2002;43:470–475. [PubMed: 11937589]
13. Fine EJ, Li Y, Blaufox MD. Parenchymal mean transit time analysis of 99mTc-DTPA captopril renography. J Nucl Med 2000;41:1627–1631. [PubMed: 11037990]
14. Szabo Z, Vosberg H, Sondhaus CA, Feinendegen LE. Model identification and estimation of organ-function parameters using radioactive tracers and the impulse-response function. European Journal of Nuclear Medicine 1985;11:265–274. [PubMed: 3908109]
15. Torsello G, Szabo Z, Vosberg H. Experimental studies on renal transfer function. Effects of renal artery stenosis and occlusion. Edizioni Minerva Medica 1985:125–127.
16. Yamashita M, Inaba T, Kawase Y, Horii H, Wakita K, Fujii R, Nakahashi H. Quantitative measurement of renal function using Ga-68-EDTA. Tohoku J Exp Med JID -0417355 1988;155:207–208.
17. Gjedde A 1995 Compartmental analysis. In: Wagner HNJr, Szabo Z, Buchanan WJ (eds). Principles of nuclear medicine. Saunders, Philadelphia:451–461

18. Logan J. Graphical analysis of PET data applied to reversible and irreversible tracers. Nucl Med Biol 2000;27:661–670. [PubMed: 11091109]
19. Nitzsche EU, Choi Y, Killion D, Hoh CK, Hawkins RA, Rosenthal JT, Buxton DB, Huang SC, Phelps ME, Schelbert HR. Quantification and parametric imaging of renal cortical blood flow in vivo based on Patlak graphical analysis. Kidney Int 1993;44:985–996. [PubMed: 8264158]
20. Gjedde A, Wong DF, Wagner HN 1985 Transient analysis of irreversible and reversible tracer binding in human brain. In: Battistin L, Gerstenbrand F (eds). PET and NMR. New perspectives in neuroimaging and in clinical neurochemistry. Alan R. Liss, INC., New York:223–235
21. Patlak CS, Blasberg RG, Fenstermacher JD. Graphical evaluation of blood-to-brain transfer constants from multiple-time uptake data. J Cereb Blood Flow Metab 1983;3:1–7. [PubMed: 6822610]
22. Szabo Z, Kao PF, Burns HD, Gibson RE, Hamill TG, Ravert HT, Kim SE, Mathews WB, Musachio JL, Scheffel U, Dannals RF. Investigation of angiotensin II/AT1 receptors with carbon-11-L-159,884: a selective AT1 antagonist. J Nucl Med 1998;39:1209–1213. [PubMed: 9669396]
23. Hutchins GD. What is the best approach to quantify myocardial blood flow with pet? J Nucl Med 2001;42:1183–1184. [PubMed: 11483677]
24. Mullani NA, Ekas RD, Marani S, Kim EE, Gould KL. Feasibility of measuring first pass extraction and flow with rubidium-82 in the kidneys. Am J Physiol Imaging JID - 8610225 1990;5:133–140.
25. Tamaki N, Rabito CA, Alpert NM, Yasuda T, Correia JA, Barlai-Kovach M, Kanke M, Dragotakes SC, Strauss HW. Serial analysis of renal blood flow by positron tomography with rubidium-82. Am J Physiol JID - 0370511 1986;251:H1024–H1030.
26. Young H, Carnochan P, Zweit J, Babich J, Cherry S, Ott R. Evaluation of copper(II)-pyruvaldehyde bis (N-4-methylthiosemicarbazone) for tissue blood flow measurement using a trapped tracer model. Eur J Nucl Med 1994;21:336–341. [PubMed: 8005157]
27. Shelton ME, Green MA, Mathias CJ, Welch MJ, Bergmann SR. Assessment of regional myocardial and renal blood flow with copper-PTSM and positron emission tomography. Circulation 1990;82:990–997. [PubMed: 2394015]
28. Young H, Carnochan P, Zweit J, Babich J, Cherry S, Ott R. Tissue blood flow estimation with copper (II)-pyruvaldehyde bis (N-4-methylthiosemicarbazone) and PET. Journal of Nuclear Biology and Medicine 2002;38(Suppl 1):89–91.
29. Killion D, Nitzsche E, Choi Y, Schelbert H, Rosenthal JT. Positron emission tomography: a new method for determination of renal function. J Urology 1993;150:1064–1068.
30. Goethals P, Volkaert A, Vandewielle C, Dierckx R, Lameire N. 55Co-EDTA for renal imaging using positron emission tomography (PET): a feasibility study. Nucl Med Biol JID - 9304420 2000;27:77–81.
31. Karanikas G, Becherer A, Wiesner K, Dudczak R, Kletter K. ACE inhibition is superior to angiotensin receptor blockade for renography in renal artery stenosis. Eur J Nucl Med Mol Imaging 2002;29:312–318. [PubMed: 12002704]
32. Clorius JH, Hupp T, Zuna I, Schmidlin P, Denk S, Van Kaick G. The exercise renogram and its interpretation. J Nucl Med 1997;38:1146–1151. [PubMed: 9225809]
33. Imanishi M, Yano M, Okumura M, Kimura G, Kawano Y, Oda J, Hayashida K, Ishida Y, Takamiya M, Omae T. Aspirin renography in diagnosis of unilateral renovascular hypertension. Hypertens Res 1998;21:209–213. [PubMed: 9786606]
34. Shreve P, Chiao PC, Humes HD, Schwaiger M, Gross MD. Carbon-11-acetate PET imaging in renal disease. J Nucl Med 1995;36:1595–1601. [PubMed: 7658216]
35. Oyama N, Miller TR, Dehdashti F, Siegel BA, Fischer KC, Michalski JM, Kibel AS, Andriole GL, Picus J, Welch MJ. 11C-acetate PET imaging of prostate cancer: detection of recurrent disease at PSA relapse. J Nucl Med 2003;44:549–555. [PubMed: 12679398]
36. Kotzerke J, Volkmer BG, Glatting G, Van Den HJ, Gschwend JE, Messer P, Reske SN, Neumaier B. Intraindividual comparison of [11C]acetate and [11C]choline PET for detection of metastases of prostate cancer. Nuclearmedizin 2003;42:25–30.
37. Seltzer MA, Jahan SA, Sparks R, Stout DB, Satyamurthy N, Dahlbom M, Phelps ME, Barrio JR. Radiation dose estimates in humans for (11)C-acetate whole-body PET. J Nucl Med 2004;45:1233–1236. [PubMed: 15235071]

38. Nabulsi NB, Smith DE, Kilbourn MR. [(11)C]Glycylsarcosine: synthesis and in vivo evaluation as a PET tracer of PepT2 transporter function in kidney of PepT2 null and wild-type mice. Bioorg Med Chem 2005;13:2993–3001. [PubMed: 15781409]
39. Han HK, Amidon GL. Targeted prodrug design to optimize drug delivery. AAPS PharmSci 2000;2:E6. [PubMed: 11741222]
40. Terada T, Inui K. Peptide transporters: structure, function, regulation and application for drug delivery. Curr Drug Metab 2004;5:85–94. [PubMed: 14965252]
41. Nielsen CU, Brodin B. Di/tri-peptide transporters as drug delivery targets: regulation of transport under physiological and patho-physiological conditions. Curr Drug Targets 2003;4:373–388. [PubMed: 12816347]
42. Theis S, Knutter I, Hartrodt B, Brandsch M, Kottra G, Neubert K, Daniel H. Synthesis and characterization of high affinity inhibitors of the H+/peptide transporter PEPT2. J Biol Chem 2002;277:7287–7292. [PubMed: 11751927]
43. Padhy AK, Solanki KK, Bomanji J, Chaiwatanarat T, Nimmon CC, Britton KE. Clinical evaluation of 99mTc diaminocyclohexane, a renal tubular agent with cationic transport: results in healthy human volunteers. Nephron 1993;65:294–298. [PubMed: 8247196]
44. Wild D, Macke HR, Waser B, Reubi JC, Ginj M, Rasch H, Muller-Brand J, Hofmann M. 68Ga-DOTANOC: a first compound for PET imaging with high affinity for somatostatin receptor subtypes 2 and 5. Eur J Nucl Med Mol Imaging 2005;32:724. [PubMed: 15551131]
45. Prakash S, Went MJ, Blower PJ. Cyclic and acyclic polyamines as chelators of rhenium-186 and rhenium-188 for therapeutic use. Nucl Med Biol 1996;23:543–549. [PubMed: 8832713]
46. Jones-Wilson TM, Deal KA, Anderson CJ, McCarthy DW, Kovacs Z, Motekaitis RJ, Sherry AD, Martell AE, Welch MJ. The in vivo behavior of copper-64-labeled azamacrocyclic complexes. Nucl Med Biol 1998;25:523–530. [PubMed: 9751418]
47. Yoo J, Reichert DE, Kim J, Anderson CJ, Welch MJ. A potential Dubin-Johnson syndrome imaging agent: synthesis, biodistribution, and microPET imaging. Mol Imaging 2005;4:18–29. [PubMed: 15967123]
48. Paulusma CC, Kool M, Bosma PJ, Scheffer GL, ter Borg F, Scheper RJ, Tytgat GN, Borst P, Baas F, Oude Elferink RP. A mutation in the human canalicular multispecific organic anion transporter gene causes the Dubin-Johnson syndrome. Hepatology 1997;25:1539–1542. [PubMed: 9185779]
49. Sun X, Kim J, Martell AE, Welch MJ, Anderson CJ. In vivo evaluation of copper-64-labeled monooxo-tetraazamacrocyclic ligands. Nucl Med Biol 2004;31:1051–1059. [PubMed: 15607487]
50. Heilig CW, Brosius FC III, Henry DN. Glucose transporters of the glomerulus and the implications for diabetic nephropathy. Kidney Int Suppl 1997;60:S91–S99. [PubMed: 9285909]
51. Wright EM. Renal Na(+)-glucose cotransporters. Am J Physiol Renal Physiol 2001;280:F10–F18. [PubMed: 11133510]
52. Bormans GM, Van Oosterwyck G, de Groot TJ, Veyhl M, Mortelmans L, Verbruggen AM, Koepsell H. Synthesis and biologic evaluation of (11)c-methyl-d-glucoside, a tracer of the sodium-dependent glucose transporters. J Nucl Med 2003;44:1075–1081. [PubMed: 12843224]
53. de Groot TJ, Veyhl M, Terwinghe C, Vanden BV, Dupont P, Mortelmans L, Verbruggen AM, Bormans GM, Koepsell H. Synthesis of 18F-fluoroalkyl-beta-D-glucosides and their evaluation as tracers for sodium-dependent glucose transporters. J Nucl Med 2003;44:1973–1981. [PubMed: 14660724]
54. Shirota K, Kato Y, Suzuki K, Sugiyama Y. Characterization of novel kidney-specific delivery system using an alkylglucoside vector. J Pharmacol Exp Ther 2001;299:459–467. [PubMed: 11602655]
55. Hwang DR, Eckelman WC, Mathias CJ, Petrillo EWJ, Lloyd J, Welch MJ. Positron-labeled angiotensin-converting enzyme (ACE) inhibitor: fluorine-18-fluorocaptopril. Probing the ACE activity in vivo by positron emission tomography. J Nucl Med JID - 0217410 1991;32:1730–1737.
56. Markham J, McCarthy TJ, Welch MJ, Schuster DP. In vivo measurements of pulmonary angiotensin-converting enzyme kinetics. I. Theory and error analysis. J Appl Physiol JID - 8502536 1995;78:1158–1168.
57. Schuster DP, McCarthy TJ, Welch MJ, Holmberg S, Sandiford P, Markham J. In vivo measurements of pulmonary angiotensin-converting enzyme kinetics. II. Implementation and application. J Appl Physiol JID - 8502536 1995;78:1169–1178.

58. Matarrese M, Salimbeni A, Turolla EA, Turozzi D, Moresco RM, Poma D, Magni F, Todde S, Rossetti C, Sciarrone MT, Bianchi G, Kienle MG, Fazio F. 11C-Radiosynthesis and preliminary human evaluation of the disposition of the ACE inhibitor [11C]zofenoprilat. Bioorg Med Chem 2004;12:603–611. [PubMed: 14738971]
59. Akcay A, Sezer S, Ozdemir FN, Arat Z, Atac FB, Verdi H, Colak T, Haberal M. Association of the genetic polymorphisms of the renin-angiotensin system and endothelial nitric oxide synthase with chronic renal transplant dysfunction. Transplantation 2004;78:892–898. [PubMed: 15385810]
60. Kaschina E, Unger T. Angiotensin AT1/AT2 receptors: regulation, signalling and function. Blood Press 2003;12:70–88. [PubMed: 12797627]
61. Nickenig G, Strehlow K, Roeling J, Zolk O, Knorr A, Bohm M. Salt induces vascular AT1 receptor overexpression in vitro and in vivo. Hypertension 1998;31:1272–1277. [PubMed: 9622141]
62. Strehlow K, Wassmann S, Bohm M, Nickenig G. Angiotensin AT1 receptor overexpression in hypercholesterolaemia. Ann Med 2000;32:386–389. [PubMed: 11028685]
63. Sodhi CP, Kanwar YS, Sahai A. Hypoxia and high glucose upregulate AT1 receptor expression and potentiate ANG II-induced proliferation in VSM cells. Am J Physiol Heart Circ Physiol 2003;284:H846–H852. [PubMed: 12433659]
64. Dumont EC, Rafrafi S, Laforest S, Drolet G. Involvement of central angiotensin receptors in stress adaptation. Neuroscience 1999;93:877–884. [PubMed: 10473253]
65. Wu Z, Maric C, Roesch D, Zheng W, Verbalis JG, Sandberg K. Estrogen regulates adrenal angiotensin type 1 receptors by modulating AT1 receptor translation. Endocrinology 2003;144:3251–3261. [PubMed: 12810582]
66. Harrison-Bernard LM, Schulman IH, Raij L. Postovariectomy hypertension is linked to increased renal AT1 receptor and salt sensitivity. Hypertension 2003;42:1157–1163. [PubMed: 14610098]
67. Nickenig G, Roling J, Strehlow K, Schnabel P, Bohm M. Insulin induces upregulation of vascular AT1 receptor gene expression by posttranscriptional mechanisms. Circulation 1998;98:2453–2460. [PubMed: 9832492]
68. Nickenig G, Bohm M. Regulation of the angiotensin AT1 receptor expression by hypercholesterolemia. Eur J Med Res 1997;2:285–289. [PubMed: 9233901]
69. Aneja A, El Atat F, McFarlane SI, Sowers JR. Hypertension and obesity. Recent Prog Horm Res 2004;59:169–205. [PubMed: 14749502]
70. Prasad A, Quyyumi AA. Renin-angiotensin system and angiotensin receptor blockers in the metabolic syndrome. Circulation 2004;110:1507–1512. [PubMed: 15364819]
71. Ortlepp JR, Breuer J, Eitner F, Kluge K, Kluge R, Floege J, Hollweg G, Hanrath P, Joost HG. Inhibition of the renin-angiotensin system ameliorates genetically determined hyperinsulinemia. Eur J Pharmacol 2002;436:145–150. [PubMed: 11834258]
72. Julius S, Kjeldsen SE, Weber M, Brunner HR, Ekman S, Hansson L, Hua T, Laragh J, McInnes GT, Mitchell L, Plat F, Schork A, Smith B, Zanchetti A. Outcomes in hypertensive patients at high cardiovascular risk treated with regimens based on valsartan or amlodipine: the VALUE randomised trial. Lancet 2004;363:2022–2031. [PubMed: 15207952]
73. Chertin B, Rolle U, Cascio S, McDermot M, O'Briain S, Farkas A, Puri P. Upregulation of angiotensin II receptors in reflux nephropathy. J Pediatr Surg 2002;37:251–255. [PubMed: 11819209]
74. Mento PF, Pica ME, Hilepo J, Chang J, Hirsch L, Wilkes BM. Increased expression of glomerular AT1 receptors in rats with myocardial infarction. Am J Physiol 1998;275:H1247–H1253. [PubMed: 9746472]
75. Modrall JG, Quinones MJ, Frankhouse JH, Hsueh WA, Weaver FA, Kedes L. Upregulation of angiotensin II type 1 receptor gene expression in chronic renovascular hypertension. J Surg Res 1995;59:135–140. [PubMed: 7630117]
76. Nickenig G. Central role of the AT(1)-receptor in atherosclerosis. J Hum Hypertens 2002;16 (Suppl 3):S26–S33. [PubMed: 12140725]
77. Kim SE, Scheffel U, Szabo Z, Burns HD, Gibson RE, Ravert HT, Mathews WB, Hamill TG, Dannals RF. In vivo labeling of angiotensin II receptors with a carbon-11-labeled selective nonpeptide antagonist. J Nucl Med 1996;37:307–311. [PubMed: 8667067]

78. Mathews WB, Yoo SE, Lee SH, Scheffel U, Rauseo PA, Zober TG, Gocco G, Sandberg K, Ravert HT, Dannals RF, Szabo Z. A novel radioligand for imaging the AT1 angiotensin receptor with PET. Nuclear Medicine and Biology 2004;31:571–574. [PubMed: 15219274]
79. Szabo Z, Speth RC, Brown PR, Kerenyi L, Kao PF, Mathews WB, Ravert HT, Hilton J, Rauseo P, Dannals RF, Zheng W, Lee S, Sandberg K. Use of positron emission tomography to study AT1 receptor regulation in vivo. J Am Soc Nephrol 2001;12:1350–1358. [PubMed: 11423564]
80. Gibson RE, Beauchamp HT, Fioravanti C, Brenner N, Burns HD. Receptor binding radiotracers for the angiotensin II receptor: radioiodinated [Sar1, Ile8]Angiotensin II. Nucl Med Biol 1994;21:593–600. [PubMed: 9234316]
81. Owonikoko TK, Fabucci ME, Brown PR, Nisar N, Hilton J, Mathews WB, Ravert HT, Rauseo P, Sandberg K, Dannals RF, Szabo Z. *In vivo* investigation of estrogen regulation of adrenal and renal angiotensin (AT1) receptor expression by PET. J Nucl Med 2003;45:94–100. [PubMed: 14734680]
82. Goodfriend TL. Angiotensin receptors: history and mysteries. Am J Hypertens 2000;13:442–449. [PubMed: 10821350]
83. de Gasparo M, Catt KJ, Inagami T, Wright JW, Unger T. International union of pharmacology. XXIII. The angiotensin II receptors. Pharmacol Rev 2000;52:415–472. [PubMed: 10977869]
84. Hamill TG, Burns HD, Dannals RF, Mathews WB, Musachio JL, Ravert HT, Naylor EM. Development of [^{11}C]L-159,884: a radiolabelled, nonpeptide angiotensin II antagonist that is useful for angiotensin II, AT1 receptor imaging. Applied Radiation and Isotopes 1996;47:211–218. [PubMed: 8852629]
85. Hong KW, Kim CD, Lee SH, Yoo SE. The in vitro pharmacological profile of KR31080, a nonpeptide AT1 receptor antagonist. Fundam Clin Pharmacol 1998;12:64–69. [PubMed: 9523186]
86. Lee BH, Seo HW, Kwon KJ, Yoo SE, Shin HS. In vivo pharmacologic profile of SK-1080, an orally active nonpeptide AT1-receptor antagonist. Journal of Cardiovascular Pharmacology 1999;33:375–382. [PubMed: 10069671]
87. Owonikoko TK, Fabucci ME, Brown PR, Nisar N, Hilton J, Mathews WB, Ravert HT, Rauseo P, Sandberg K, Dannals RF, Szabo Z. *In vivo* investigation of estrogen regulation of adrenal and renal angiotensin AT1 receptor expression by PET. J Nucl Med 2003;45:94–100. [PubMed: 14734680]
88. Guyton AC, Coleman TG, Manning RD, Hall JE. Some problems and solutions for modeling overall cardiovascular regulation. Mathematical Biosciences 1984;72:141–155.
89. Anderson WP, Ramsey DE, Takata M. Development of hypertension from unilateral renal artery stenosis in conscious dogs. Hypertension 1990;16:441–451. [PubMed: 2210812]
90. Tsuji Y, Goldfarb DA, Masaki Z, Ferrario CM. Patterns of renal function in hypertension due to unilateral renal artery occlusion. Clin Exp Hypertens A 1992;14:1067–1081. [PubMed: 1358485]
91. Admiraal PJ, Danser AH, Jong MS, Pieterman H, Derkx FH, Schalekamp MA. Regional angiotensin II production in essential hypertension and renal artery stenosis. Hypertension 1993;21:173–184. [PubMed: 8428780]
92. Mai M, Hilgers KF, Wagner J, Mann JFE, Geiger H. Expression of angiotensin-converting enzyme in renovascular hypertensive rat kidney. Hypertension 1995;25:674–678X. [PubMed: 7721414]
93. Haefliger JA, Bergonzelli G, Waeber G, Aubert JF, Nussberger J, Gavras H, Nicod P, Waeber B. Renin and angiotensin II receptor gene expression in kidneys of renal hypertensive rats. Hypertension 1995;26:733–737. [PubMed: 7591011]
94. Wilkes BM, Pion I, Sollott S, Michaels S, Kiesel G. Intrarenal renin-angiotensin system modulates glomerular angiotensin receptors in the rat. American Journal of Physiology 1988;254:F345–F350. [PubMed: 3348413]
95. Lu XY, Li XM, Li LY, Li L, Li CL, Wang HY. Variation of intrarenal angiotensin II and angiotensin II receptors by acute renal ischemia in the aged rat. Renal Failure 1996;18:19–29. [PubMed: 8820498]
96. Regitz-Zagrosek V, Neuss M, Holzmeister J, Warnecke C, Fleck E. Molecular biology of angiotensin receptors and their role in human cardiovascular disease. J Mol Med 1996;74:233–251. [PubMed: 8773261]
97. Ernst CB, Daugherty ME, Kotchen TA. Relatonship between collateral development and renin in experimental renal artery stenosis. Surgery 1976;80:252–258. [PubMed: 941096]

98. Llorens-Cortes C, Greenberg B, Huang H, Corvol P. Tissular expression and regulation of type 1 angiotensin II receptor subtypes by quantitative reverse transcriptase-polymerase chain reaction analysis. Hypertension 1994;24:538–548. [PubMed: 7525476]
99. Unger T. The role of the renin-angiotensin system in the development of cardiovascular disease. The American Journal of Cardiology 2002;89:3A–9A.
100. Schieffer B, Schieffer E, Hilfiker-Kleiner D, Hilfiker A, Kovanen PT, Kaartinen M, Nussberger J, Harringer W, Drexler H. Expression of angiotensin II and interleukin 6 in human coronary atherosclerotic plaques: potential implications for inflammation and plaque instability. Circulation 2000;101:1372–1378. [PubMed: 10736279]
101. Pantuck AJ, Berger F, Zisman A, Nguyen D, Tso CL, Matherly J, Gambhir SS, Belldegrun AS. CL1-SR39: A noninvasive molecular imaging model of prostate cancer suicide gene therapy using positron emission tomography. J Urol 2002;168:1193–1198. [PubMed: 12187266]
102. Textor SC. Ischemic nephropathy: where are we now? J Am Soc Nephrol 2004;15:1974–1982. [PubMed: 15284283]
103. Gerhard A, Schwarz J, Myers R, Wise R, Banati RB. Evolution of microglial activation in patients after ischemic stroke: a [11C](R)-PK11195 PET study. Neuroimage 2005;24:591–595. [PubMed: 15627603]
104. Jemal A, Tiwari RC, Murray T, Ghafoor A, Samuels A, Ward E, Feuer EJ, Thun MJ. Cancer statistics, 2004. CA Cancer J Clin 2004;54:8–29. [PubMed: 14974761]
105. Pantuck AJ, Zisman A, Belldegrun AS. The changing natural history of renal cell carcinoma. J Urol 2001;166:1611–1623. [PubMed: 11586189]
106. Chow WH, Devesa SS, Warren JL, Fraumeni JF Jr. Rising incidence of renal cell cancer in the United States. Journal of American Medical Association 1999;281:1628–1631.
107. Sorger D, Patt M, Kumar P, Wiebe LI, Barthel H, Seese A, Dannenberg C, Tannapfel A, Kluge R, Sabri O. [18F]Fluoroazomycinarabinofuranoside (18FAZA) and [18F]Fluoromisonidazole (18FMISO): a comparative study of their selective uptake in hypoxic cells and PET imaging in experimental rat tumors. Nucl Med Biol 2003;30:317–326. [PubMed: 12745023]
108. Rasey JS, Grunbaum Z, Magee S, Nelson NJ, Olive PL, Durand RE, Krohn KA. Characterization of radiolabeled fluoromisonidazole as a probe for hypoxic cells. Radiat Res 1987;111:292–304. [PubMed: 3628717]
109. Rasey JS, Koh WJ, Evans ML, Peterson LM, Lewellen TK, Graham MM, Krohn KA. Quantifying regional hypoxia in human tumors with positron emission tomography of [18F]fluoromisonidazole: a pretherapy study of 37 patients. Int J Radiat Oncol Biol Phys 1996;36:417–428. [PubMed: 8892467]
110. Koh WJ, Rasey JS, Evans ML, Grierson JR, Lewellen TK, Graham MM, Krohn KA, Griffin TW. Imaging of hypoxia in human tumors with [F-18]fluoromisonidazole. Int J Radiat Oncol Biol Phys 1992;22:199–212. [PubMed: 1727119]
111. Fujibayashi Y, Taniuchi H, Yonekura Y, Ohtani H, Konishi J, Yokoyama A. Copper-62-ATSM: a new hypoxia imaging agent with high membrane permeability and low redox potential. J Nucl Med 1997;38:1155–1160. [PubMed: 9225812]
112. Gronroos T, Eskola O, Lehtio K, Minn H, Marjamaki P, Bergman J, Haaparanta M, Forsback S, Solin O. Pharmacokinetics of [18F]FETNIM: a potential marker for PET. J Nucl Med 2001;42:1397–1404. [PubMed: 11535732]
113. Evans SM, Kachur AV, Shiue CY, Hustinx R, Jenkins WT, Shive GG, Karp JS, Alavi A, Lord EM, Dolbier WR Jr, Koch CJ. Noninvasive detection of tumor hypoxia using the 2-nitroimidazole [18F] EF1. J Nucl Med 2000;41:327–336. [PubMed: 10688119]
114. Rajendran JG, Wilson DC, Conrad EU, Peterson LM, Bruckner JD, Rasey JS, Chin LK, Hofstrand PD, Grierson JR, Eary JF, Krohn KA. [(18)F]FMISO and [(18)F]FDG PET imaging in soft tissue sarcomas: correlation of hypoxia, metabolism and VEGF expression. Eur J Nucl Med Mol Imaging 2003;30:695–704. [PubMed: 12632200]
115. Dolbier WR Jr, Li AR, Koch CJ, Shiue CY, Kachur AV. [18F]-EF5, a marker for PET detection of hypoxia: synthesis of precursor and a new fluorination procedure. Applied Radiation and Isotopes 2001;54:73–80. [PubMed: 11144255]

116. Nishikibe M, Ohta H, Okada M, Ishikawa K, Hayama T, Fukuroda T, Noguchi K, Saito M, Kanoh T, Ozaki S, Kamei T, Hara K, William D, Kivlighn S, Krause S, Gabel R, Zingaro G, Nolan N, O'Brien J, Clayton F, Lynch J, Pettibone D, Siegl P. Pharmacological properties of J-104132 (L-753,037), a potent orally active, mixed ET_A/AT_B endothelin receptor antagonist. Journal of Pharmacology and Experimental Therapeutics 1999;289:1262–1270. [PubMed: 10336515]

117. Aleksic S, Szabo Z, Scheffel U, Ravert HT, Mathews WB, Vaterlein O, Kerenyi L, Gibson RE, Ryan C, Hamill T, Burns HD, Dannals RF. In vivo labeling of endothelin receptors with [^{11}C] L-735,037: Studies in mice and a dog. J Nucl Med 2001;42:1274–1280. [PubMed: 11483691]

118. Chen X, Tohme M, Park R, Hou Y, Bading JR, Conti PS. Micro-PET imaging of alphavbeta3-integrin expression with 18F-labeled dimeric RGD peptide. Mol Imaging 2004;3:96–104. [PubMed: 15296674]

119. Haubner R, Weber WA, Beer AJ, Vabuliene E, Reim D, Sarbia M, Becker KF, Goebel M, Hein R, Wester HJ, Kessler H, Schwaiger M. Noninvasive visualization of the activated alphavbeta3 integrin in cancer patients by positron emission tomography and [18F]Galacto-RGD. PLoS Med 2005;2:e70. [PubMed: 15783258]

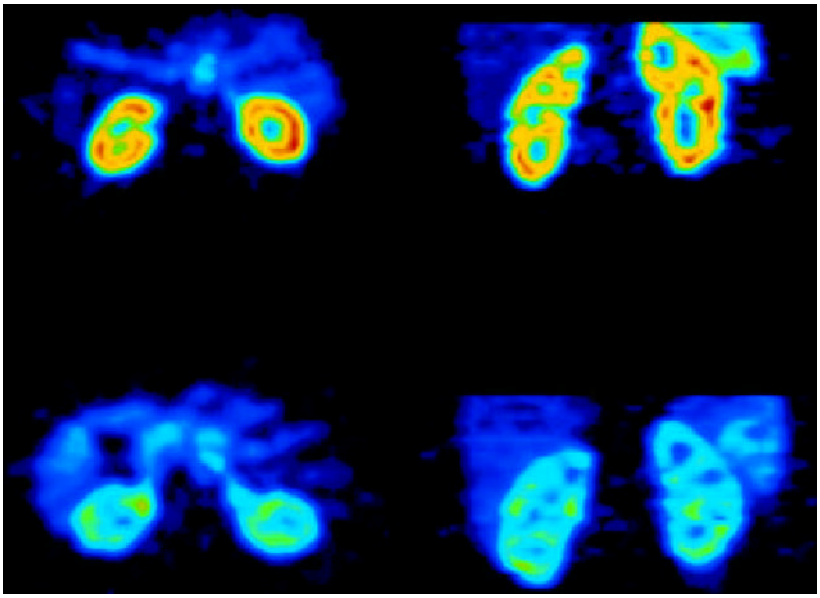

Figure 1.
Renal blood flow images obtained with O-15 water in a healthy subject (upper row) and in a subject with renal insufficiency (lower row).
(Reproduced with permission, Alpert et al. 2002).

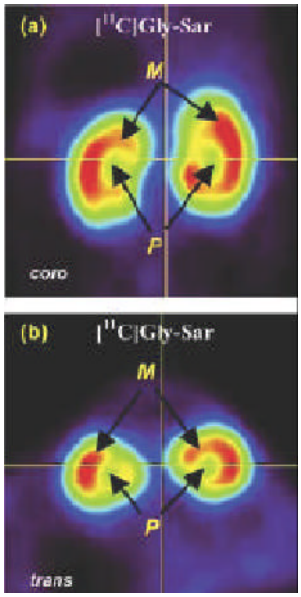

Figure 2.
Small animal PET images of the renal peptide transporter obtained with the dipeptide C-11 Gly-Sar
(Reproduced with permission, Nabulsi et al. 2005).

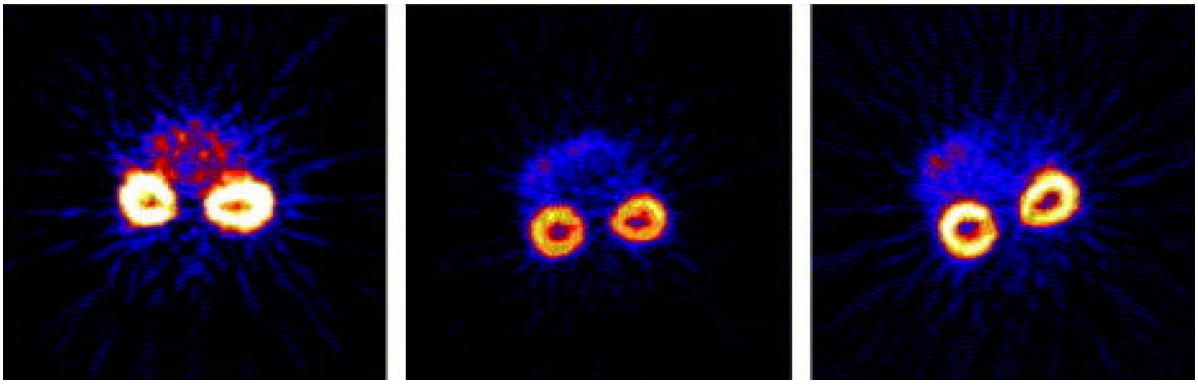

Figure 3.
Renal accumulation of Cu-64 monooxo-tetraazamacrocyclic ligands (Reproduced with permission, Sun et al. 2004).

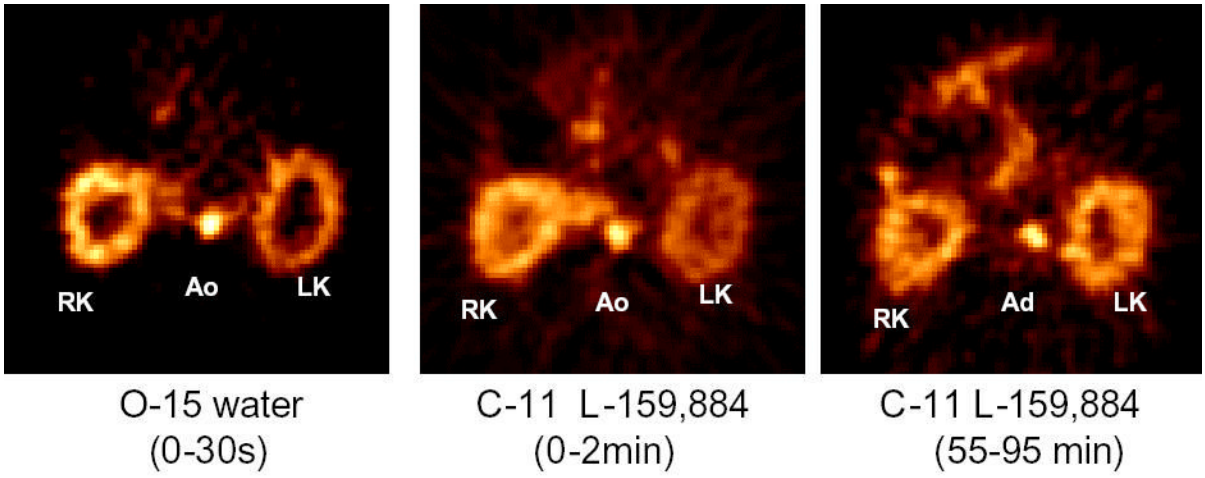

Figure 4.

Images of the kidneys of a dog with experimental renovascular hypertension (left sided renal artery stenosis). Both O-15 water (left hand side image) and the early accumulation of the AT1R specific tracer C-11 L-159,884 (middle image) demonstrate decreased perfusion of the left kidney. Delayed images of C-11 L-159,884 retention (right hand side image) indicate increased receptor binding.

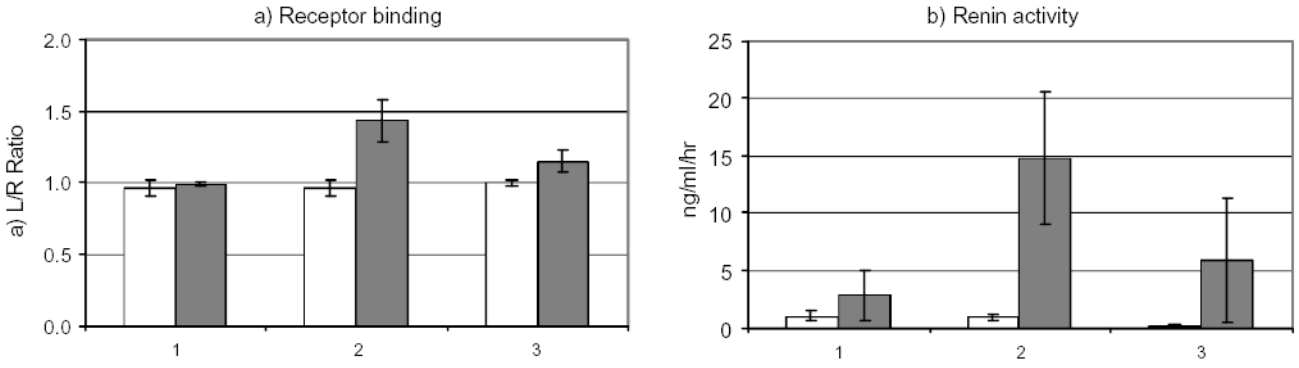

Figure 5.

AT1R receptor binding (left) and renin activity in dogs at baseline (1), acute renal artery stenosis (2) and chronic renal artery stenosis (3). Open squares represent control animals (n=2), dark squares represent animals with renal artery stenosis (n=4). Increased receptor binding correlates with increased plasma renin activity during acute renal artery stenosis. In chronic renal artery stenosis receptor binding and renin activity are increased but to a lesser degree than in acute renal artery stenosis.

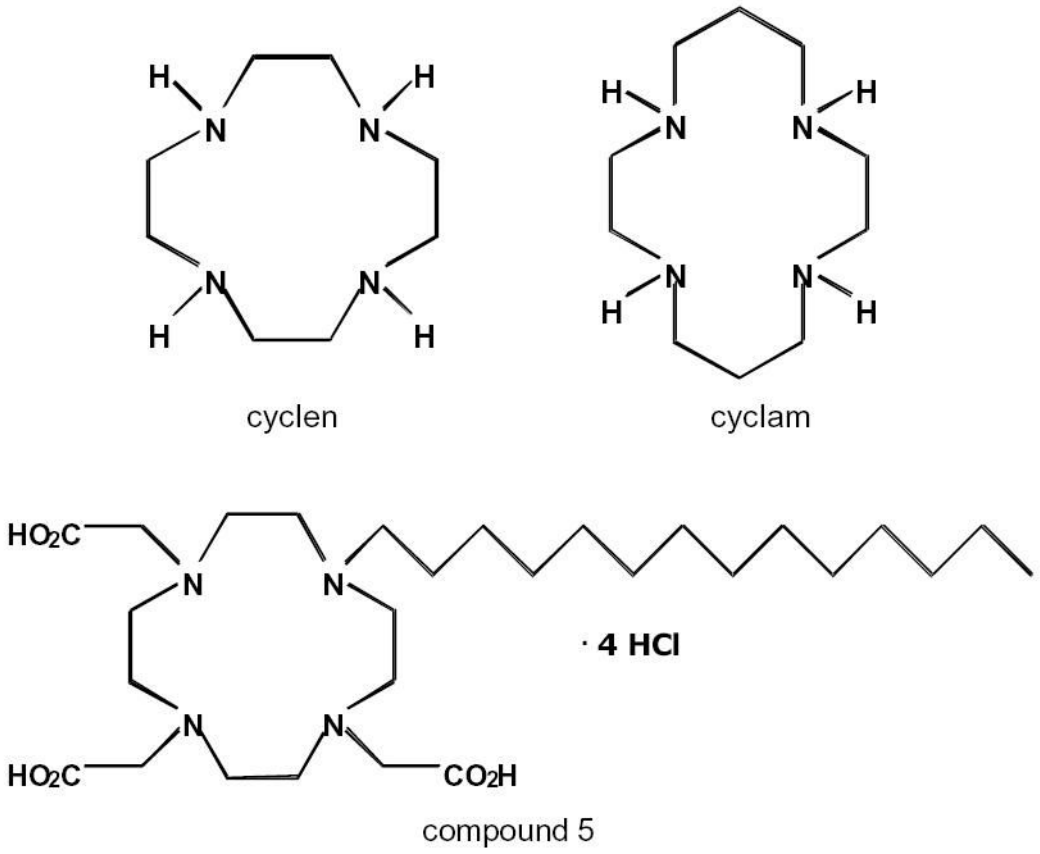

Scheme 1.
Chemical Structure of cyclen, cyclam, and 1,4,7,10-tetraazacyclododecane hydrochloride salt or compound 5 in (Yoo et al. 2005). Compound 5 is the substrate of the hepatic cMOAT transporter.

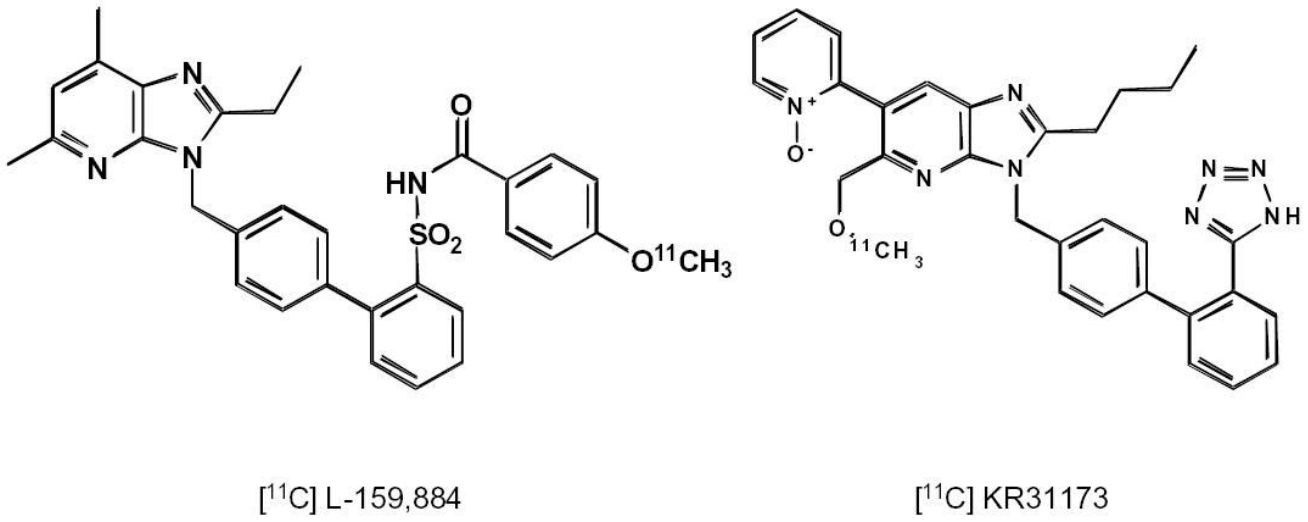

[11C] L-159,884 [11C] KR31173

Scheme 2.
Chemical structures of C-11 L-159,884 and C-11 KR31173.

Tables

	Isotope	T1/2	E($^{+}$max)
	Rb-82	75 sec	3.35 MeV
	O-15	2 min	1.72 MeV
10 min N-13	Cu-62	9.7 min	2.9 MeV